

# Experimental study of the modulational instability of intense plasma waves in a plasma

Yu. Ya. Brodskii, A. G. Ditvak, Ya. Z. Slutsker, and G. M. Fraïman

*Institute of Applied Physics, Academy of Sciences of the USSR*

(Submitted 27 June 1990)

Zh. Eksp. Teor. Fiz. **100**, 159–172 (July 1991)

The modulational instability of plasma waves excited in an isotropic plasma by an electron beam has been studied experimentally. This instability leads to the formation of quasisteady three-dimensional cavities. The plasma-wave field trapped in these cavities is not cut off from the pump.

## 1. INTRODUCTION

Strong Langmuir turbulence is an interesting aspect of nonlinear plasma physics. The incontestable progress which has been made in theoretical work on this problem has stimulated some special model experiments designed for studying the basic microscopic processes which determine the dynamics of intense plasma waves (Langmuir waves) in an isotropic plasma.

There is a long list of theoretical papers on the evolution of the modulational instability and on accompanying effects: the formation and evolution of solitons and cavitons and collapse processes (see, for example, Refs. 1–5 and the bibliographies there). Possible steady states and the dynamics of intense wave packets have been studied.

On the experimental side, unfortunately, the number of studies is considerably smaller (see Refs. 6–13 and the bibliographies there). Some interesting results obtained in these experiments can be explained in terms of the onset of the modulational instability. Among these effects are the following:

- a) the excitation of collapsing spikes of the Langmuir field<sup>10,11</sup> and a change in the plasma density matched with the field,
- b) the formation of long-lived, quasi-one-dimensional structures (cavitons),<sup>12</sup> and
- c) the appearance of superthermal electrons and the distortion of the original plasma distribution function.<sup>13</sup>

Several important questions, on the other hand, have not been studied adequately. For example, the roles played by the pumping and the damping in the modulational instability and in shaping of the steady-state distributions (of solitons and cavitons) remain essentially unexplained. There has been little study of questions concerning the transverse stability of solitons and the stabilization of collapse in an isotropic plasma. Furthermore, the polarization of the Langmuir field in the cavities as these cavities evolve has not been studied experimentally.

In this paper we are reporting a study undertaken to learn about these topics. These experiments had some special aspects. First, we used an unconventional method to excite the plasma waves in the plasma. This method involved the introduction of static electric fields in the volume in which the electron beam interacted with the plasma. This approach made it possible to control the intensity of the plasma waves and their growth rate.<sup>14,15</sup> We should stress that we used a hot-cathode plasma source and multipole magnetic insulation of the walls. Sources of this type have an emit-

ting cathode at a negative potential with respect to the plasma. In other words, plasma waves may be excited as an internal property of such plasma sources.<sup>15</sup> A second important aspect of this study concerns the particular conditions selected for the excitation of the plasma waves. From the very outset, the spatial distribution of the field amplitude was that of a localized quasimonochromatic spike with a single maximum.

Before we present the basic results, we think it useful to briefly review some qualitative aspects of the mechanism by which the plasma waves were excited and pumped in our experiments. This question was discussed in detail in Ref. 15.

The localized quasimonochromatic Langmuir-field spikes observed experimentally can be excited if a static electric field acts on the electron beam. A qualitative explanation for this result is that (in contrast with the situation without a static field) there is a change in the time spent by the beam electrons in the retarding and accelerating phases of the rf field. The expression for the behavior of the beam energy  $Q$  during the interaction with the plasma field  $E(x)\sin\omega t$  in the presence of a static field  $E_0(x) = -\partial U/\partial x$  can be described formally (under the same approximations as are used in the derivation of the equations describing Landau damping) by

$$Q = \int v_0 f(v_0) \Delta J(v_0) dv_0,$$

$$\Delta J = \frac{1}{2} \frac{\partial}{\partial J_0} |J_{\sim}|^2, \quad J_{\sim} = \int_0^l eE(x) e^{i\omega t(x)} dx,$$

$$J_0 = \frac{mv_0^2}{2} = \frac{mv^2}{2} - eU(x), \quad t(x) = \int_0^x \frac{dx}{v(x)}.$$

Here  $\Delta J(v_0)$  is an average over the entrance phase of the change in the energy of an electron beam (this is the change in the energy of a single electron, averaged over entrance phase; the beam is of unit density and is monoenergetic at the entrance);  $f(v_0)$  is the electron velocity distribution at the entrance; and  $t(x)$  is the average over the entrance phase of the transit time of an electron to a given point in the interaction volume, determined with allowance for the static field.

From these relations, and ignoring the effect of the static field on the transit time ( $t = x/v_0$ ), we see that the sign of  $\Delta J$  is determined by the derivative of the intensity of the spatial Fourier spectrum:

$$\Delta J \sim -\frac{\partial}{\partial k} |E_k|^2 \quad \text{for} \quad k = \frac{\omega}{v_0}.$$

If this quantity is strictly positive, a beam with an arbitrary distribution function would thus be incapable of exciting a spike of this sort. If the electrons are instead moving in a nonuniform way on the average, the result will depend strongly on the change in the transit angle  $[\omega t(x)]$  with respect to the unperturbed value  $(\omega x/v_0)$ .

If, for example, the rf field distribution in the spike has a single scale [e.g.,  $\exp(-x^2/a^2)$  or  $1/\cosh(x/a)$ ], then we have  $\Delta J(v_0) > 0$  in the absence of a static field. In other words, pumping would not be possible at any electron energy. If we instead impose a static electric field, then the times spent by an electron in the accelerating and retarding phases of the field change, so changes occur in the processes by which energy is exchanged between the beam and the rf field. Incorporating a static field is formally equivalent to taking up the problem of the interaction of a beam in uniform motion (in the absence of a static field) with an effective rf field

$$E_{eff}(x) = E(x) \exp\left\{i\left[\omega t(x) - \omega \frac{x}{v_0}\right]\right\}$$

whose spectrum depends on  $U(x)$  and is consistent with the appearance of regions with  $\Delta J(v_0) < 0$ , i.e., excitation zones.

The results reported below can be interpreted successfully on the basis of this model. The plasma waves are at first excited efficiently by the electron beam on the given plasma density profile by a voltage applied between the cathode and the anode (this may be a static or pulsed voltage). In the next stage, when the waves have reached a sufficient amplitude, ponderomotive forces begin to act on the field and plasma distributions. Processes corresponding to the nonlinear stage of the modulational instability become important at this point.

## 2. EXPERIMENTAL APPARATUS AND DIAGNOSTICS

The design and construction of the apparatus are described in detail in Ref. 15. The plasma is produced in a hot-cathode discharge, with multipole magnetic insulation of the chamber walls. The diameter of the discharge chamber is 40 cm, and its length is 35 cm. The pressure of the neutral gas (xenon) is  $(2-4) \cdot 10^{-5}$  torr. The steady-state plasma den-

sity is in the interval  $(5-8) \cdot 10^8 \text{ cm}^{-3}$ . The relative beam density is 1-3%. The static anode voltage can be varied over the range 50-150 V; it has essentially no effect on the plasma density. The electron temperature  $T_e$  is 8-10 eV.

We would like to point out some structural features of this apparatus (Fig. 1).

a) In place of peripheral cathodes there is a flat frame cathode  $10 \times 10$  cm in size consisting of 11 tungsten filaments 0.12 mm in diameter connected in parallel. The cathode is near one end of the chamber, on the axis of the chamber, outside the magnetic field near the wall.

b) An auxiliary anode, a metal disk 10 cm in diameter, is positioned near the end of the chamber opposite the cathode, again on the axis of the chamber and outside the magnetic field. This anode is connected to the main anode (the chamber wall) through the winding of a pulse transformer. This winding has a low dc resistance, which can be ignored in steady-state operation. A square voltage pulse with a height up to 1.5 kV and a length up to  $10 \mu\text{s}$ , with rise and decay times of 200-250 ns, can be applied to the auxiliary anode.

These modifications were made to the apparatus in order to produce a one-dimensional, directed beam of emitted electrons through the plasma. Direct measurements showed that the auxiliary anode captured  $\sim 50\%$  of the emitted electrons in steady-state operation, while during the application of a pulsed voltage the corresponding figure was essentially 100%. The dimensions of the region occupied by the Langmuir field increased, since conditions were more favorable for the onset of the modulational instability.

The strength of the rf electric field and the plasma density are measured simultaneously, by the same movable single Langmuir probe. The operation of the probe of this sort as a receiving antenna for plasma waves was discussed in Ref. 16. The high-frequency component of the output current from the probe (the component near the plasma frequency  $\omega_p$ ) and the low-frequency component (below the ion plasma frequency  $\omega_{pi}$ ) are separated. The low-frequency component is fed directly to an oscilloscope, while the high-frequency component is either rectified and then sent to the oscilloscope or studied with a spectrum analyzer.

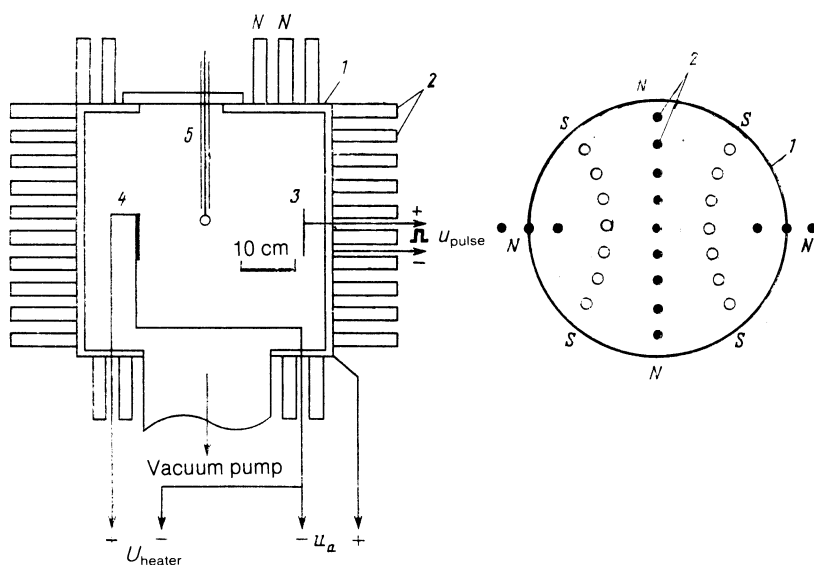


FIG. 1. Schematic diagram of the apparatus. 1—Vacuum chamber; 2—magnets; 3—auxiliary anode; 4—plane cathode; 5—movable antenna;  $U_{pulse}$ —square voltage pulse.

A constant bias voltage (of about 30 V) is applied to the probe to keep it operating in the regime of a saturation ion current. The diameter of this probe ( $d_p = 5$  mm) was chosen to strike a compromise between the requirements of high spatial resolution (a minimal value of  $d_p$ ) and a satisfactory shape of the probe characteristic (with a well-expressed region of a saturation ion current). This is a necessary condition for measurements of the plasma density  $n_e$  ( $d_p \gg r_d \approx 0.1$  cm, where  $r_d$  is the electron Debye length).

Polarization measurements of the Langmuir field are carried out with a special movable antenna. This antenna is a miniature symmetric dipole. Its characteristic dimensions (0.1 cm) are shorter than the electron Debye length. The polarization sensitivity of this miniature antenna is greater than 30 dB, so it is completely suitable for measuring the direction of the Langmuir field. Unfortunately, this miniature antenna is not suitable for simultaneous measurements of the plasma density, because of its small collecting surface area.

Important information about the interaction of the electric field with the plasma is embodied in the electron velocity distribution or the electron energy distribution and the dynamics of either distribution. To study the electron velocity distribution we used the Druyvesteyn method, which is based on the circumstance that the electron energy distribution is proportional to the second derivative of the current-voltage characteristic found with the help of a single Langmuir probe.<sup>17</sup> This method made it possible to measure the distribution function in 2–3  $\mu$ s.

### 3. EXPERIMENTAL RESULTS

By manipulating the steady-state plasma density, the anode voltage, and the height of the high-voltage pulse on the auxiliary anode, we were able to vary not only the steady-state strength of the Langmuir field but also its rate of increase. This is a very important point, since this rate of increase directly affects the dynamics of the modulational instability.

One can clearly distinguish two types of application of the Langmuir field. They might be called "fast" and "slow" applications. The time scale for the application of the field in the fast case is much shorter than the time over which ion sound propagates over the length scales of the field, while in the slow regime the application time is longer than the ion acoustic time. The fast application is achieved by applying a high-voltage pulse to the auxiliary anode when the plasma has a density selected to make the pulse height correspond to the middle of the excitation zone (since the pulse was short, the plasma could not undergo any substantial changes). In this case, intense plasma waves appear during the application of the pulse. However, the high-voltage pulse could also be used to apply the Langmuir field smoothly, if we made use of the slow (ion-acoustic) global movement of the plasma after the end of the pulse. This movement is caused by the pulse. In the course of this motion, the region in which steady-state excitation occurs in the absence of a pulse becomes deformed. This deformation in turn changes the angle at which the electrons traverse this region and thus the excitation intensity. The most intense plasma waves and the greatest changes in the plasma density occur after the end of the pulse.

We turn now to the experimental results. We will discuss the cases of fast and slow application of the Langmuir field separately.

**3.1. Fast application.** To excite the plasma waves, we applied a high-voltage pulse ( $U_{\text{pulse}} \sim 1.5$  kV) with a short rise time ( $\tau_r \sim 0.2$   $\mu$ s) to the auxiliary anode. We chose the steady-state value of the plasma density  $n_e$  to correspond, at the selected value of  $U_{\text{pulse}}$ , to the maximum strength of the Langmuir field,  $E_l$  (the middle of the excitation zone).

The measurements showed that the intensity of the plasma waves was spatially nonuniform and varied over time. Figure 2 shows the evolution of the spatial distribution of the amplitude of the plasma waves. We see that as early as 1  $\mu$ s after the beginning of the pulse (this is when the measurements were begun) a clearly defined double-hump distribution of the amplitude has formed. The maxima are in a plane parallel to the plane of the cathode. The typical dimensions of one maximum are 1.5–2 cm. Control measurements showed that the field distribution was not azimuthally symmetric. The length scale of a maximum along the direction perpendicular to the plane of Fig. 2 (parallel to the plane of the cathode) was 1.5–2 cm; i.e., the field distribution corresponded to two "spikes," rather than to a torus.

As time elapsed, the maximum field amplitude fell off slowly, and the relative depth of the valley between the two maxima increased. Then came a sharp decrease in the field amplitude. The width of the field spikes increased. The spikes merged, and the field distribution became a single-hump distribution with typical sizes of 3–4 cm.

The maximum value of the Langmuir field was 150–200 V/cm. Figure 3 shows the distribution of the electric field lines at the maximum field strength.

Unfortunately, because of the low sensitivity of the miniature antenna, measurements could not be carried out at low field amplitudes. It can be seen from Fig. 3 that the field lines near the cathode are essentially perpendicular to the plane of the cathode. With distance from the cathode, the field lines begin to rotate, and they simultaneously move closer together (i.e., the field increases). Near the field maximum the field lines are rotated 60–80° from their original direction. With distance from the cathode, the angle through which the field line rotates remains large, but the field itself becomes much weaker.

The experimental results reported above depend on only the parameters of the pulse and the value of  $n_e$ . They are essentially independent of the static anode voltage and, correspondingly, independent of the level of steady-state excitation of plasma waves in the absence of the pulse. The absence of a detailed picture of the rise and evolution of the Langmuir field to its maximum value is a shortcoming of this series of experiments. Another shortcoming is the inability to measure the plasma density during the pulse, because the probe surface is being bombarded with electrons with an energy  $\sim 1.5$  keV. To some extent, the experiments with a smooth application of the pump field are not afflicted with these problems. We turn now to that case.

**3.2 Slow application.** The steady-state values of the plasma density  $n_e$  and the anode voltage were chosen such that the amplitude of the spike was at a maximum after the application of the high-voltage pulse. Simultaneous measurements of the dynamics of  $E_l$  and  $n_e$  showed that there is a

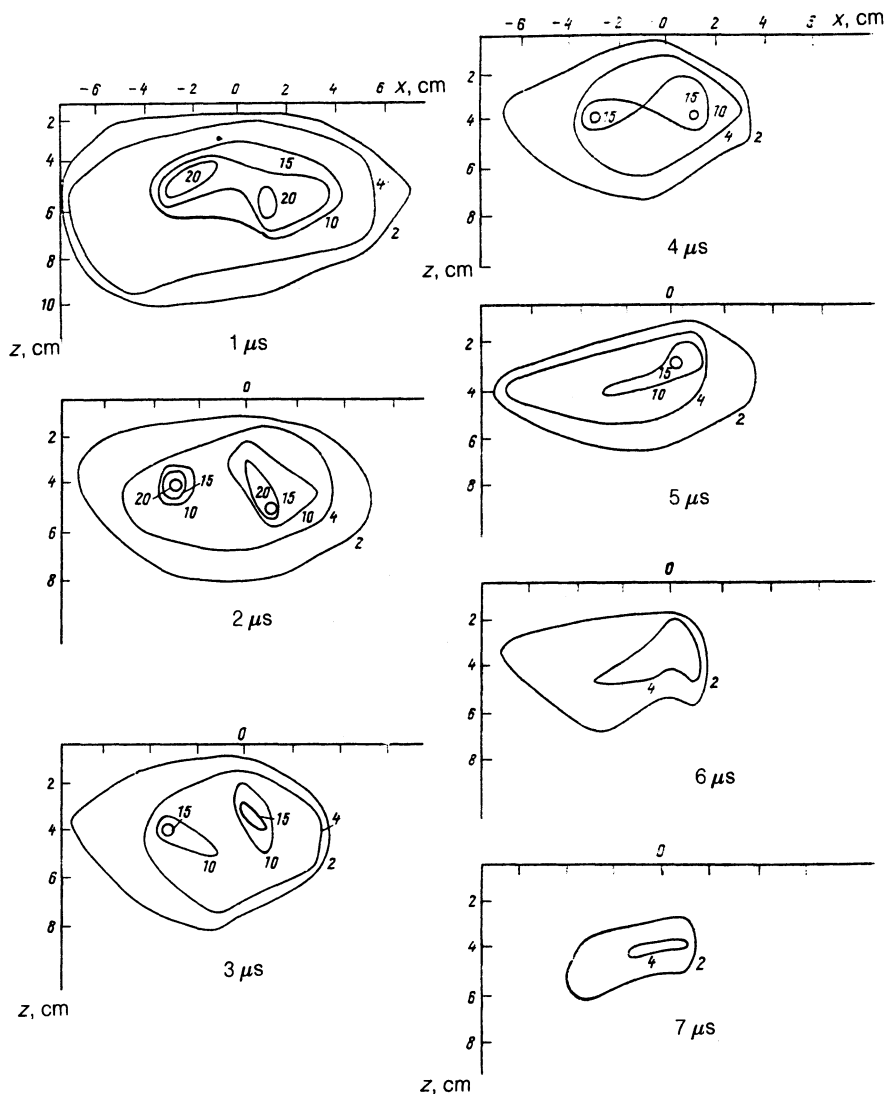


FIG. 2. Evolution of the spatial distribution of the Langmuir field during fast application in the plane perpendicular to the cathode, passing through the middle of the cathode. The  $x$  axis lies in the plane of the cathode. Here  $z$  is the distance from the cathode. The contour curves are labeled with the field  $E$ , in units of  $10 \text{ V/cm}$ .

clear correlation between the field spike and the dip in the density  $n_e$  in the region of maximum field. Figure 4 shows the space-time evolution of the Langmuir field and of the plasma density. Here the origin for the time scale is the end of the high-voltage pulse. The rate at which the field and density were measured in this series of experiments was substantially lower than in the case of the fast application of a

field. In the present case, the time interval between two successive pictures of the spatial distribution of  $E_l$  is  $10 \mu\text{s}$  (Fig. 4), in contrast with the  $1 \mu\text{s}$  in the previous case (Fig. 2).

After the pump pulse, the field amplitude is initially low, and the field distribution is a slightly asymmetric pancake in the plane parallel to the plane of the cathode. The profile of  $n_e$  is a slightly asymmetric plateau tilting toward the cathode. As time elapses, and the Langmuir field increases, reaching  $30\text{--}40 \text{ V/cm}$  (this was the maximum value attainable under steady-state conditions), the region with the field begins to break up in the direction perpendicular to the original density gradient. At the same time, the contour curves of the density in the field intensification region also begin to move apart from each other; density dips appear. In addition, we detect a slight global movement of the plasma away from the cathode. Later on, when the Langmuir field reaches its maximum value of  $90\text{--}100 \text{ V/cm}$  (at  $\sim 30 \mu\text{s}$  in this time scale), the distribution of the field becomes double-humped with a length scale of  $2\text{--}3 \text{ cm}$ . In the maximum-field region we see some clearly defined density dips, with a depth reaching  $20\text{--}25\%$ .

As time elapses, the field thus decreases, moving back toward its original value. The depth of the density dips de-

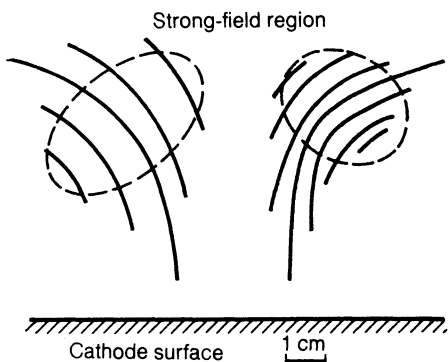


FIG. 3. Polarization of the electric field in the spikes.

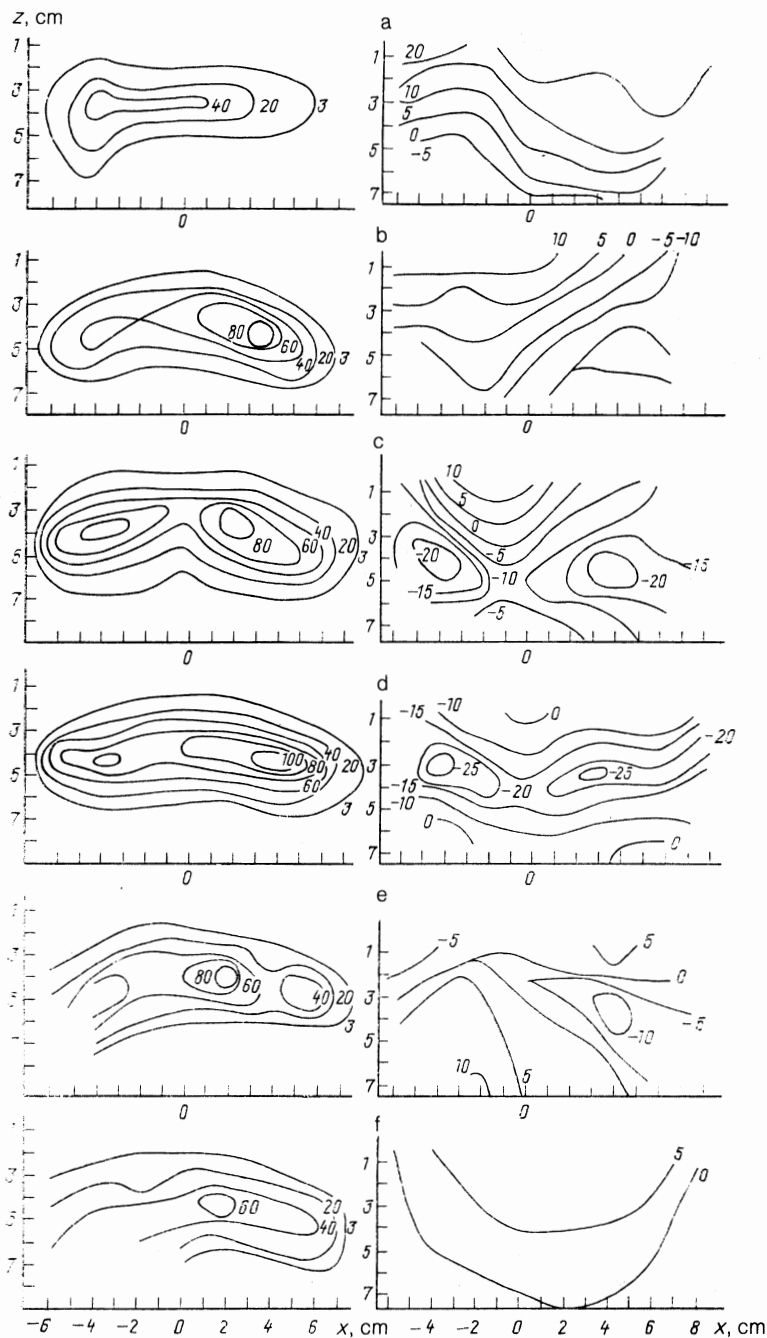


FIG. 4. Space-time evolution of the Langmuir field and the plasma density during the slow application of the pump. a—10  $\mu$ s after the end of the field spike; b—20; c—30; d—40; e—50; f—60  $\mu$ s. The contour curves in the frames at the left are labeled with the absolute value of the field in volts per centimeter. The contour curves in the frames at the right are labeled with the change in density (as a percentage) from its original value (a minus sign on a number means a density decrease).

creases, and after about 60  $\mu$ s the plasma becomes essentially homogeneous. The humps also disappear from the spatial distribution of the field.

The spectral measurements showed that the frequency of the plasma waves at the time of the spike decreased by 7–10%.

Figure 5 shows the relative depth of a density dip,  $\delta n_e/n_e$ , versus the quantity  $E_1^2/(16\pi n_e T_e)$ . We see that above a threshold field of 30–40 V/cm the plot of  $\delta n_e/n_e$  versus  $E_1^2$  is essentially linear.

Figure 6, a and b, shows electron energy distributions at a low electric field and at the time of the spike, respectively. We see that when the field is weak the energy of the bulk of

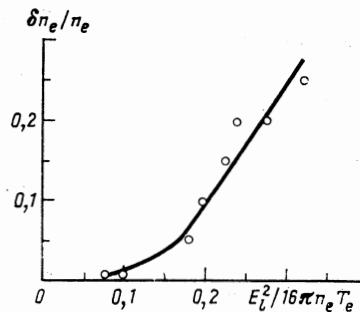


FIG. 5. Magnitude of the dip in the density in a cavity versus the intensity of the Langmuir field.

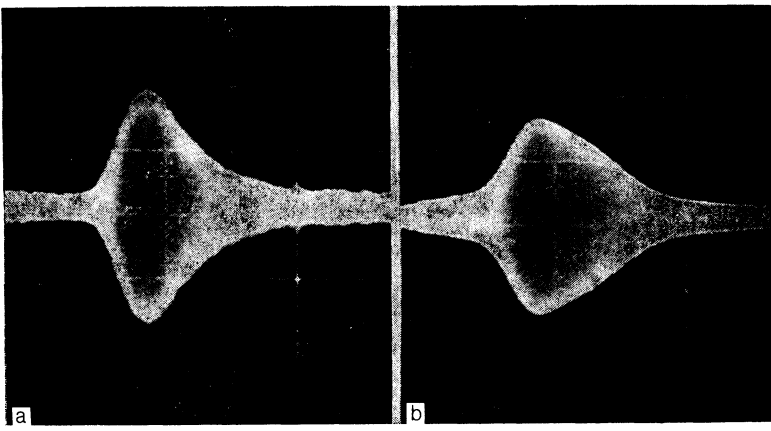


FIG. 6. Electron energy distributions. a—Before the application of a pulse; b—during the field spike. The horizontal scale is 10 eV/div.

the electrons does not exceed 10 eV. This situation is characteristic of steady-state excitation. At the time of the spike, when the length scales of the field are at a minimum, while the field itself is at a maximum, there is an additional increase in the energy of the plasma electrons (this energy roughly doubles), and the electron energy distribution acquires a shape different from its original shape.

#### 4. DISCUSSION OF RESULTS

We will first discuss the results obtained during the rapid application of the high voltage:  $\tau_r \lesssim 0.2 \mu\text{s} \ll l/v_s$ . Here  $l \sim 7 \text{ cm}$  is the initial length scale of the Langmuir field, and  $v_s \sim 3 \cdot 10^5 \text{ cm/s}$  is the ion acoustic velocity. Let us estimate the time over which the Langmuir field increases to its maximum value  $E_{\text{max}}$  as a result of the “monotron” excitation mechanism. Direct measurements showed that  $E_{\text{max}}$  reached 200 V/cm. The time taken by the field to rise to this value can be described by

$$\tau = \gamma_m^{-1} \ln(E_{\text{max}}/E_{\text{therm}}).$$

Here  $\gamma_m$  is the maximum growth rate of the monotron instability, which is given by the following expression, as was shown in Ref. 15:

$$\gamma_m \approx 4\pi^2 \frac{n_b}{n_e} \frac{v_b}{l}. \quad (1)$$

Substituting in the values  $n_b/n_e \approx 3 \cdot 10^{-2}$ ,  $v_b = (2eU_{\text{pulse}}/m)^{1/2} = 2.3 \cdot 10^9 \text{ cm/s}$ , and  $l = 7 \text{ cm}$ , we find  $\gamma_m \approx 4 \cdot 10^8 \text{ s}^{-1}$ . Using

$$E_{\text{therm}}^2/8\pi n_e T_e \sim (n_e r_d^3)^{-1}$$

to estimate the size of the thermal fluctuations of the Langmuir field, we find  $E_{\text{therm}} \approx 0.15 \text{ V/cm}$ . The rise time of the Langmuir field,  $\tau$ , is then  $\sim 0.2 \mu\text{s}$ . Since the measurements began 1  $\mu\text{s}$  after the field was applied, we can assert that the amplitude of the rf field managed to reach its maximum value  $E_{\text{max}}$ .

The varying fields which arise are easily capable of changing the density by means of the ponderomotive force [an estimate of the ponderomotive force from the formula  $E_{\text{st}} = (16\pi n_e T_e)^{1/2}$  yields a value  $\sim 180 \text{ V/cm} \approx E_{\text{max}}$ ]. A varying large-amplitude Langmuir field can lead to the formation of local cavities, to the formation of solitons, or to collapse processes via the modulational instability.

If collisional losses are ignored, we have the following

expression for the threshold for the modulational instability:<sup>1,2</sup>

$$\frac{E_{\text{thr}}^2}{16\pi n_e T_e} \geq (kr_d)^2, \quad (2)$$

where  $k \approx 2\pi/l$ , and  $l$  is the length scale of the field. Under our experimental conditions, the initial length scales of the variations were 6–7 cm, as can be seen from Fig. 2. The pump level was  $E^2/(16\pi n_e T_e) \approx 1$ , and the condition  $l \gg r_d \approx 0.1 \text{ cm}$  held. In other words, the field was well above the threshold for the onset of the modulational instability. The scale achieved for the instability, however, is not the optimum scale calculated for a uniform field, because of the nonuniformity of the pump field. Collisional losses are being ignored here since the corresponding threshold fields,

$$\frac{E_{\text{thr}}^2}{16\pi n_e T_e} \geq \frac{\nu}{\omega_p} \quad (3)$$

are substantially lower than those found from (2). In other words, dispersion effects are more important. Here  $\nu \approx 2 \cdot 10^5 \text{ s}^{-1}$  is the collision rate, and  $\omega_p$  is the electron plasma frequency.

Note that in this case we are dealing with the transverse breakup of the original large-scale field distribution (“transverse” here means transverse with respect to the direction of the electron beam and, at least, the original direction of the Langmuir field).<sup>2)</sup>

A deformation of the field in the directions transverse with respect to the beam was also observed at high pump levels in the experiments of Refs. 10 and 13. The occurrence of a “transverse” instability in our experiments, without a “longitudinal” instability, is a consequence of the small longitudinal dimensions of the region occupied by the Langmuir field and the rapid increase in Landau damping as this dimension decreases. The transverse dimensions of this region are larger than the longitudinal dimensions, so the limitation which we mentioned above on the onset of the modulational instability for the transverse direction does not operate. The modulational instability gives rise to variations on the originally smooth transverse structure of the field. The length scale of these variations is also determined by the onset of Landau damping.

Unfortunately, a distinct collapse of plasma waves was not observed in these experiments, although the threshold for the modulational instability was surpassed. The reason

was the small "starting" dimensions of the spikes of the Langmuir field. Because of this, Landau damping prevented any significant decrease in the regions occupied by the rf field.

The growth rate of the modulational instability in the case of strong fields can be written in the form<sup>1,2</sup>

$$\gamma \approx 2\omega_p \left( \frac{E_r^2 m}{16\pi n_e T_e M} \right)^{1/2}. \quad (4)$$

Here  $m$  is the mass of an electron, and  $M$  a mass of an ion. The condition for the applicability of expression (4),

$$E_r^2 / 16\pi n_e T_e > m/M,$$

is satisfied by a wide margin under our experimental conditions. Substituting numerical values into (4), we find  $\gamma \approx 7 \cdot 10^6 \text{ s}^{-1}$ . Consequently, the rise time of the modulational instability is  $\tau = \gamma^{-1} \approx 0.1\text{--}0.2 \mu\text{s}$ . Consequently, at the time the observations began ( $1 \mu\text{s}$  at the beginning of the pulse) we were in the initial stage of the development of the modulational instability: with two humps on the field profile.

Later, during the second and third microseconds, the modulational instability continues to develop: The ratio  $E_{\text{max}}/E_{\text{min}}$  increases. By the end of this process, at 3 or 4  $\mu\text{s}$ , the modulation depth is at a maximum. The minimum length scale of the field,  $l_m \sim 1.5 \text{ cm}$ , is related to the level of the Langmuir field by (2), as can easily be seen by substituting in the numerical values of  $l_m$  and  $E_r$ .

We can assert that the comparatively slow evolution of the local fields observed here is a consequence of a dynamic equilibrium between the supply of energy by the electron beam (which excites the field) and the energy removal by Landau damping at sharp local variations in the field, i.e., the quasisteady dissipative structures realized in these experiments.<sup>19</sup> The importance of considering both the generation and the dissipation of energy was confirmed by the observation that a rapid removal of the pump resulted in an essentially instantaneous (on the scale of the pulse length) disappearance of the field irregularities due to the Landau damping (a "burn-up" of the field<sup>18</sup>). The Landau damping rate can be written<sup>20</sup>

$$\frac{\gamma_L}{\omega_p} = \left( \frac{\pi}{8} \right)^{1/2} \frac{e^{-\eta}}{(kr_d)^3} \exp\left( -\frac{1}{2(kr_d)^2} \right). \quad (5)$$

Substituting the numerical values of  $r_d$  (even if we ignore a possible increase in  $T_e$ ) and  $k = 2\pi/l_m$  into this expression, we find a damping time  $\tau = \gamma_L^{-1} \approx 0.1 \mu\text{s}$ . We are ignoring collisional losses here because they are small ( $\nu \sim 10^5 \text{ s}^{-1}$ ). We thus see that the field in a cavity is not cut off from the pump in this case (the same comment apparently applies to Ref. 21), because of the short damping time.

The rise time of this double-humped structure,  $\sim 3 \mu\text{s}$ , corresponds to the time taken by ion sound ( $v_s \approx 3 \cdot 10^5 \text{ cm/s}$ ) to traverse the distance between the humps. The smooth decrease in the amplitude of the waves which were excited during the pump pulse was apparently caused by degradation of the generation conditions, because of a deviation of the transit angle from the optimum value. This deviation was a consequence of the global movement of the plasma caused by the high potential applied to the auxiliary anode.

Later, 4–5  $\mu\text{s}$  after the application of the pump pulse, the maximum field amplitude continues to decrease. The local maxima of the field broaden and become smoother, forming a wide, single-humped structure (Fig. 2). The time scale of this coalescence is the ion acoustic time and could only be related to an accompanying redistribution of the density.

Another argument supporting the idea that plasma cavities form is the rotation of the field lines of the Langmuir field in the regions in which the maxima of this field localize. The reason is that the change in the direction of the field lines of the rf field is associated with a change in the dielectric constant  $\epsilon$  of the plasma, i.e., a change in the plasma density. If a field line is incident at an angle  $\theta_1$  on a boundary between two media, with  $\epsilon_1$  and  $\epsilon_2$ , the angle  $\theta_2$  by which this field line will deviate from the normal in the second medium is given by

$$\text{tg } \theta_2 = \frac{\epsilon_2}{\epsilon_1} \text{tg } \theta_1. \quad (6)$$

In the case  $\epsilon_2 < \epsilon_1$  we would have  $\theta_2 < \theta_1$ .

The deviation of the field lines from the normal in our experiments could thus be explained only on the basis of an increase in the dielectric constant of the plasma and therefore a decrease in its density in the strong-field region. A similar rotation of field lines will be observed when cavities appear in a totally homogeneous plasma.

We would like to summarize the basic disadvantages of experiments in which a pump field is applied rapidly. (a) The rapid application of the pump prevents observation of the onset of the modulational instability in its early stages, in which its growth rate is at a maximum. (b) Under these conditions it is not possible to study the dynamics of the plasma density, because the probe surface is bombarded with high-energy electrons.

We turn now to the results obtained when the pump field is applied smoothly. We recall that in this case the measurements were carried out after the end of the high-voltage pulse.

The initially uniform distribution of the field and the density begins to break up ( $10 \mu\text{s}$  after the end of the pulse) when a threshold value  $E_{\text{thr}} = 30 \text{ V/cm}$  is reached. In contrast with the preceding experiments, the threshold in this case is quite obvious (Fig. 5), and its value corresponds well to the threshold for the modulational instability, (2). Substituting the numerical values ( $k = 2\pi/l$ ,  $l = 6\text{--}7 \text{ cm}$ ,  $n_e = 7 \cdot 10^8 \text{ cm}^{-3}$ , and  $T_e = 15 \text{ eV}$ ) into this expression, we find a threshold field  $E_{\text{thr}} = 30 \text{ V/cm}$ . As in the preceding case, the collisional damping has no strong effect on the threshold. The size of the density dip,  $\delta n_e/n_e$ , agrees well with the value determined from the high-frequency electric field [ $E^2/(16\pi n_e T_e) \sim \delta n_e/n_e$ ; Fig. 5].

The time scale of the variations in the field and the density here is longer than the time taken by the ion sound to propagate across the region with the field,  $\tau_s = l/v_s \lesssim 20 \mu\text{s}$ , while the entire cycle takes  $\sim 60 \mu\text{s}$  (in xenon) (i.e., this is the time taken by the sound to propagate through the entire plasma). It can thus be assumed that at each instant we obtain a quasisteady distribution of  $n_e$  corresponding to the given field (in contrast with the preceding case). The maximum value of the field here is lower than that in the fast

regime,  $E_{\max} \leq 90\text{--}100$  V/cm, and the corresponding (and measured) value of  $\delta n_e/n_e$  is 25%.

The shift which we detected in the frequency of the Langmuir field (a downward shift of 15 MHz) could in principle be explained by a local decrease of 15% in the density in the cavities. This argument agrees well with the data presented above.

The minimum size of the field spikes ( $\sim 2\text{--}3$  cm) corresponds to the onset of Landau damping, as in the preceding case. Further evidence for this conclusion comes from the broadening of the electron distribution function when the intensity of the Langmuir field reaches its maximum (Fig. 6).

## 5. CONCLUSION

Let us summarize the results of this study. The threshold for the onset of the modulational instability is determined (if collisions are ignored) by the maximum length scale of the rf field, regardless of the direction of this field.

If the time scale for the increase in the pump level is much longer than the reciprocal of the growth rate of the modulational instability, a quasisteady state is established at each instant. In this state, the density profile reproduces the field distribution precisely, and the depth of the density dip reproduces the strength and frequency shift of the Langmuir field. If the application time is instead comparable to the reciprocal of the growth rate of the modulational instability, the time scale of the field evolution is determined by the time taken by ion sound to propagate across the length scales of the rf field.

In either case, the onset of the modulational instability gives rise to quasisteady cavities. The field inside these cavities is not cut off from the pump, and the dynamics of the system consisting of the plasma and the Langmuir field is determined by the supply of energy from the pump source (the electron beam) and by the removal of energy (by Landau damping).

In the cavities, we observe a dipole field distribution with a partial asymmetry which is a consequence of the global inhomogeneity of the plasma.

The additional deformations and broadening of the electron energy distribution stem from the traversal of small-scale regions with a strong Langmuir field.

The most serious disadvantage of these experiments was that it was not possible to observe a clearly expressed self-contraction of the field. The reason for this was the small "starting" dimensions of the rf field spikes (the threshold

parameters were not exceeded to a sufficient extent). The size of the apparatus will have to be increased in order to eliminate this problem.

We wish to express our deep gratitude to M. V. Nezlin for useful discussions.

<sup>1</sup> The fact that the detector is operating in the linear regime is being taken into account here.

<sup>2</sup> The transverse instability of a "plane" soliton was studied in Ref. 18.

<sup>1</sup> V. E. Zakharov, Zh. Eksp. Teor. Fiz. **62**, 1745 (1972) [Sov. Phys. JETP **35**, 908 (1972)].

<sup>2</sup> A. G. Litvak and G. M. Fraïman, in *Interaction of Intense Electromagnetic Waves with Collisionless Plasmas* (ed. A. G. Litvak), Izd. IPF Akad. Nauk SSSR, Gorki, 1980, p. 50.

<sup>3</sup> G. M. Fraïman, Zh. Eksp. Teor. Fiz. **88**, 390 (1985) [Sov. Phys. JETP **61**, 228 (1985)].

<sup>4</sup> V. E. Zakharov, A. N. Pushkarev, A. M. Rubenchik, R. Z. Sagdeev, and V. F. Shvets, Pis'ma Zh. Eksp. Teor. Fiz. **47**, 239 (1988) [JETP Lett. **47**, 287 (1988)].

<sup>5</sup> D. L. Newman, P. A. Robinson, and M. V. Goldman, Phys. Rev. Lett. **62**, 2132 (1989).

<sup>6</sup> Yu. Ya. Brodskii, V. L. Gol'tsman, A. G. Pitvak, and S. I. Nechuev, *Interaction of Intense Electromagnetic Waves with Collisionless Plasmas* (ed. A. G. Litvak), Izd. IPF Akad. Nauk SSSR, Gorki, 1980, p. 186.

<sup>7</sup> Yu. V. Zadiraka, Candidate's Dissertation, Kiev State University, Kiev, 1986.

<sup>8</sup> K. E. Lonngren, Plasma Phys. **25**, 943 (1983).

<sup>9</sup> M. V. Nezlin, *Dynamics of Beams in Plasmas*, Energoizdat, Moscow, 1982, Chap. 8.

<sup>10</sup> P. Y. Cheung, A. Y. Wong, C. B. Darrow, and S. J. Qian, Phys. Rev. Lett. **48**, 1348 (1982).

<sup>11</sup> D. M. Karfidov, A. M. Rubenchik, K. F. Sergeichev, and I. A. Sychev, Pis'ma Zh. Eksp. Teor. Fiz. **48**, 315 (1988) [JETP Lett. **48**, 346 (1988)].

<sup>12</sup> A. Y. Wong, P. Leung, and D. Eggleston, Phys. Rev. Lett. **39**, 997 (1977).

<sup>13</sup> P. Y. Cheung and A. Y. Wong, Phys. Fluids **23**, 1538 (1985).

<sup>14</sup> Yu. Ya. Brodsky, S. I. Nechuev, Ya. Z. Slutsker, A. M. Feygin, and G. M. Freiman, *Proc. VIII ESCAMPING*, Greifswald, 1986, p. 392.

<sup>15</sup> Yu. Ya. Brodskii, S. I. Nechuev, Ya. Z. Slutsker, A. M. Feigin, and G. M. Fraïman, Fiz. Plazmy **15**, 1187 (1989) [Sov. J. Plasma Phys. **15**, 688 (1989)].

<sup>16</sup> A. A. Andronov and Yu. V. Chugunov, Usp. Fiz. Nauk **116**, 79 (1975) [Sov. Phys. Usp. **18**, 343 (1975)].

<sup>17</sup> G. M. Malyshev and V. L. Fedorov, Dokl. Akad. Nauk SSSR **92**, 269 (1953).

<sup>18</sup> V. E. Zakharov and A. M. Rubenchik, Zh. Eksp. Teor. Fiz. **65**, 997 (1973) [Sov. Phys. JETP **38**, 494 (1974)].

<sup>19</sup> V. I. Petviashvili and O. Yu. Tselodub, Fiz. Plazmy **6**, 467 (1980) [Sov. J. Plasma Phys. **6**, 257 (1980)].

<sup>20</sup> A. B. Mikhaïlovskii, *Theory of Plasma Instabilities*, Vol. 1, Atomizdat, Moscow, 1970, Chap. 1-5 (Consultants Bureau, New York, 1973).

<sup>21</sup> P. Y. Cheung and A. Y. Wong, Phys. Rev. Lett. **55**, 1880 (1985).

Translated by D. Parsons